ELSEVIER

Mathematics and Computers in Simulation 56 (2001) 585–600

MATHEMATICS AND COMPUTERS IN SIMULATION

www.elsevier.nl/locate/matcom

Embedded solitons: a new type of solitary wave

J. Yang [a], B.A. Malomed [b], D.J. Kaup [c,*], A.R. Champneys [d]

[a] *Department of Mathematics and Statistics, The University of Vermont, Burlington, VT 05401, USA*
[b] *Department of Interdisciplinary Studies, Faculty of Engineering, Tel Aviv University, Tel Aviv 69978, Israel*
[c] *Department of Mathematics, University of Central Florida, Orlando, FL 32816-6990, USA*
[d] *Department of Engineering Mathematics, University of Bristol, Bristol BS8 ITR, UK*

Abstract

We describe a novel class of solitary waves in second-harmonic-generation models with competing quadratic and cubic nonlinearities. These solitary waves exist at a discrete set of values of the propagation constants, being embedded inside the continuous spectrum of the linear system ("embedded solitons", ES). They are found numerically and, in a reduced model, in an exact analytical form too. We prove analytically and verify by direct simulations that the fundamental (single-humped) ESs are linearly stable, but are subject to a weak nonlinear one-sided instability. In some cases, the nonlinear instability is so weak that ES is a virtually stable object. Multi-humped embedded solitons are found too, all being linearly (strongly) unstable. © 2001 Published by Elsevier Science B.V. on behalf of IMACS.

Keywords: Embedded soliton; Multi-humped; Bragg gratings

1. Introduction

Gap solitons are a generic type of solitary wave which occur in various nonlinear media [1,2]. They exist if the soliton's intrinsic frequency (temporal or spatial, depending on the physical interpretation) belongs to a gap in the spectrum of the corresponding linearized system. Typically, optical gap solitons are found in models of resonant Bragg gratings equipped with various nonlinearities, such as the Kerr nonlinearity (see the review [2]), second-harmonic generation [3–5], or self-induced transparency [6–8]. Recently, it was demonstrated that another carrier for optical gap solitons is provided by an asymmetric dual-core nonlinear optical fiber, the shape of its cores being selected so that they have opposite signs of the effective dispersion [9]. Thus far, gap solitons were observed experimentally only in a short Kerr-nonlinear glass fiber (with a length of several centimeters) with a Bragg grating written on it [10].

In this work, we consider a new type of a soliton which is an isolated solitary-wave solution, residing inside the continuous spectrum of the linearized system. It is known that families of "delocalized solitons" (i.e. quasi-solitary waves with nonvanishing oscillatory tails) may exist inside the continuous spectrum.

* Corresponding author.
E-mail address: kaup@mail.ucf.edu (D.J. Kaup).

0378-4754/01/$20.00 © 2001 Published by Elsevier Science B.V. on behalf of IMACS.
PII: S0378-4754(01)00327-5

Solutions of this type were found in various models of hydrodynamic [11–17] and optical [19,20] origin. However, in certain types of nonlinear-wave systems, the amplitude of the tail can exactly vanish at a discrete set of values of the frequencies, resulting in truly localized solitary-wave solutions existing inside the continuous spectrum . We will call them embedded solitons (ES). In contrast with gap solitons, ESs usually cannot exist in continuous families, but only as isolated solutions (exceptions are also known though, see [18] and this work below). The fact that an ES is an isolated solution presents a fundamental obstacle in attempting to apply traditional analytical methods of nonlinear wave theory, such as multiscale expansions in powers of the nonlinearity and the inverse of the soliton's width. So far, ESs have been only found either numerically, or in exceptional cases, as exact analytical solutions. Below, we will demonstrate a reduced model that does admit an exact analytical ES solution.

In many cases, it can be demonstrated that fundamental (single-humped) ESs are linearly (neutrally) stable, but nonlinearly semi-stable (see Section 3 below for a more precise definition). In the most physically relevant parametric region of the model studied here, the nonlinear instability is found to be so weak that ESs are, as a matter of fact, essentially stable objects.

As a physical model which gives rise to ESs, we consider a nonlinear optical medium combining quadratic and cubic nonlinearities. Various models of this type have been recently considered in the context of competing nonlinearities in spatial optical waveguides [21,22]. We start with a rather general system, written for a temporal (rather than spatial) domain, in terms of nonlinear optics. In dimensionless variables, the model takes the form [23]

$$iu_z + \left(\tfrac{1}{2}\right) u_{tt} + u^* v + \gamma_1(|u|^2 + 2|v|^2)u = 0, \tag{1}$$

$$iv_z - \left(\tfrac{1}{2}\right) \delta v_{tt} + qv + \left(\tfrac{1}{2}\right) u^2 + 2\gamma_2(|v|^2 + 2|u|^2)v = 0. \tag{2}$$

Here, z and t are the propagation distance and reduced time, u and v are the amplitudes of the fundamental and second harmonics (FH and SH), $(-\delta)$ is the relative dispersion of SH, q is the phase mismatch between the two harmonics, and $\gamma_{1,2}$ are the Kerr (cubic) nonlinear coefficients, which are inversely proportional to the effective cross-section areas at the corresponding carrier frequencies [23]. In the spatial domain, when t plays the role of a transverse coordinate, one should set $-\delta \equiv 1/2$, which corresponds to diffraction rather than dispersion [3–5]. However, δ can have either sign in the temporal domain, $\delta > 0$ corresponding to the case when the FH and SH belong, respectively to the regions of anomalous and normal dispersion (the latter case was considered, e.g. in Ref. [24]). Note that we did not include the group-velocity terms into Eqs. (1) and (2), because, as is well known, they can be eliminated, provided that $\delta \neq -1/2$. When $\delta = -1/2$, the model (1) and (2) is Galilean invariant, which allows one to generate a whole family of "moving" solitons from the single zero-walkoff one [25]. At all other values of δ, construction of moving (nonzero-walkoff) solitons is a nontrivial problem [26,27]. A careful numerical search has failed to find moving ESs in this model for $\delta \neq -1/2$. However, we note that they have recently been found in other models with either cubic or quadratic nonlinearity [28,29].

In the case $\delta > 0$, we need to assume $\gamma_{1,2} < 0$, as it turns out that the ESs do not exist otherwise. A straightforward interpretation of the latter condition is that the cubic nonlinearity is self-defocusing. A medium of such a type could be created on the basis of organic optical materials. Alternatively, instead of Eqs. (1) and (2), one may consider their complex conjugate versions. In that case, the cubic nonlinearity becomes self-focusing, which is a more common case, but then a relatively exotic element of the model is that the dispersion must be normal for FH and anomalous for SH; nevertheless, the latter property is

possible in existing materials which have two zero-dispersion points [23]. In the case $\delta < 0$, we will need to assume $\gamma_{1,2} > 0$ to provide for the existence of ESs, which is the ordinary case in nonlinear optics.

Recent progress with the observation of the temporal (gap) solitons in second-harmonic generating optical media [30] suggests that the ESs may well be observable too. It is also noteworthy that, in fact, a weak cubic nonlinearity is sufficient to generate ESs, which is what one expects to be present in a typical material. In accord with the above observations, in the numerical simulations presented here, we will set

$$\gamma_1 = \gamma_2 = -0.05 \times \sin(\delta), \tag{3}$$

with q and δ allowed to take on arbitrary values.

It should be stressed that the present paper represents a significant extension of our previous work [31]. One of the major new results deals with the treatment of the physically significant case $\delta < 0$. ESs for the $\delta > 0$ case are also studied here in more detail, in order to uncover the parameter intervals in which they exist. In addition, we augment these new numerical results with a comprehensive analysis of a certain reduced model in the case where the SH is much weaker than the FH. For this model we detail the role of the various parameters in determining when ESs exist, and also explain the above-stated new result of why we could find no moving ESs, except in the trivial case $\delta = -1/2$, when we have Galilean invariance. But perhaps one of the most striking new results is in the $\delta < 0$ case. We not only find new ESs, but we also show that they may be much more stable than the above-mentioned semi-stability property would suggest. This result suggests the experimental observation of the ESs might indeed be feasible.

Another remark worth making is that since the original publication of [31], in addition to the system (1) and (2), ESs have been identified in a wide array of other physical systems as well (see [18,32–37]). Many of the properties we uncover for (1) and (2) would appear to also hold for these other systems. In particular, the semi-stability of fundamental ES in generalized 5th-order KdV equations was recently proved for Hamiltonian perturbations using soliton perturbation theory in [18] (note also that this generalization included nonHamiltonian perturbations where strictly stable ESs were found).

2. Existence of embedded solitons

2.1. The full model

Stationary solutions to Eqs. (1) and (2) are sought in the form $u(z,t) = U(t)\exp(ikz)$, $v(z,t) = V(t)\exp(ikz)$, where k is a real propagation constant, and U and V are real functions governed by the equations

$$\left(\tfrac{1}{2}\right)U'' - kU + U^*V + \gamma_1(|U|^2 + 2|V|^2)U = 0, \tag{4}$$

$$-\left(\tfrac{1}{2}\right)\delta V'' + (q - 2k)V + \left(\tfrac{1}{2}\right)U^2 + \gamma_2(|V|^2 + 2|U|^2)V = 0. \tag{5}$$

The linearization of Eqs. (1) and (2) generates a continuous spectrum consisting of two disconnected branches

$$k < 0 \ \text{ or } k > \tfrac{1}{2}q, \ \text{ for } \delta > 0; \ k < 0 \ \text{ or } \ k < \tfrac{1}{2}q, \ \text{ for } \ \delta < 0. \tag{6}$$

Usually it is supposed that a stationary wave with a propagation constant k belonging to the continuous spectrum cannot be localized, because the corresponding linearized equations for the soliton's tail would

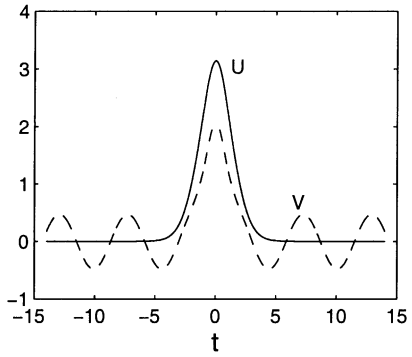

Fig. 1. The components of the delocalized soliton for $k = 0.8$. The notation where $U(t)$ is given by a solid line and $V(t)$ by a dashed one is adopted throughout this paper. Here $\delta = 1$, $q = 1$, and $\gamma_1 = \gamma_2 = -0.05$.

have nonvanishing oscillatory solutions rather than pure exponentially decaying ones. For example, when $\delta > 0$ and $k > q/2$, the propagation constant k lies in the continuous spectrum of the V component, and one may write the V-tail in the form

$$V = R(k, \phi_0) \cos\left(\sqrt{\left(\frac{2}{\delta}\right)(2k - q)}\,|t| + \phi_0\right) \quad \text{as} \quad t \to \infty \tag{7}$$

(we assume that the soliton is an even function) with an amplitude R and phase constant ϕ_0. This tail expression is valid when $R \ll 1$. The dependence $R(k, \phi_0)$ is determined by matching the linear tails (7) to the nonlinear solution of the soliton's core. Thus, one expects that the only quasi-solitary waves possible inside the continuous spectrum are delocalized solitons with the nondecaying tails. For instance, with the values $\delta = q = 1$ and $\gamma_{1,2}$ as specified in (3), $k = 0.8$ falls into the continuous spectrum (6), which gives rise to a typical delocalized soliton shown in Fig. 1.

However, due to the form of Eqs. (4) and (5), the mutually independent exponential decay of the FH and SH tails is not the only possible asymptotic solution. Concerning Eq. (4), it is clear that if U and V do vanish asymptotically, then one is always left with the linear part of the equation, hence the existence of a solution whose FH component is localized demands, in any case, that $k > 0$. However, in Eq. (5) the situation is different, depending on the relative decay rate of V and U^2 as $|t| \to \infty$. In fact, one has two generic possibilities: V vanishing slower than U^2, or exactly at the same rate as it. Here, we are interested in the latter case, when, evidently, Eq. (5) may not be linearized. This possibility of the asymptotic locking of the tails' decay rates, leading to the nonlinearizability of the SH equation, has been noted earlier (see, e.g. [38]).

A remarkable feature revealed by systematic numerical simulations is that, nevertheless, the purely quadratic nonlinearity does not give rise to ESs in the present model: another necessary ingredient is the cubic nonlinearity. Specifically, it was found that Eqs. (1) and (2) without the cubic terms (or with self-focusing ones, $\gamma_{1,2} > 0$, at $\delta > 0$) generate only the delocalized solitons inside the continuous spectrum, whose tails in the SH component never vanish. Moreover, both the simulations and an analytical variational approximation have shown that the gap in the model without the cubic terms is completely empty, containing no gap solitons (we do not present details to illustrate this negative result).

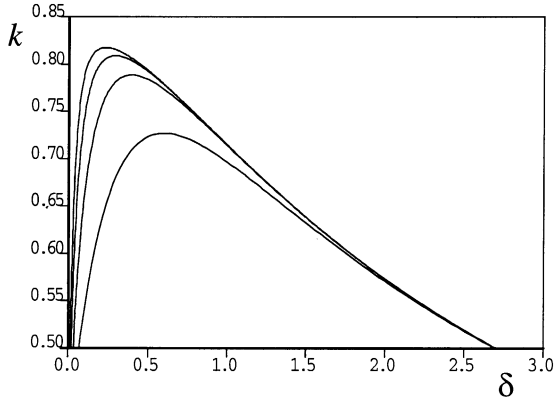

Fig. 2. Branches of the embedded solitons for positive values of δ and $q = 1$. The fundamental branch is the inner one.

Let us start by describing the results for $\delta > 0$. Simulating Eqs. (4) and (5) with the self-defocusing cubic terms (3) we have found that, at certain discrete values of k lying inside the continuous spectrum (6), the amplitude of the V-tail indeed exactly vanishes (while the U-component is localized for all positive values of k), so that the delocalized soliton becomes a true ES. In Fig. 2, the embedded-soliton solution branches for positive δ and $q = 1$ are shown in the (δ, k) plane. The numerical results suggest that there is an infinite number of such branches, only four of them being displayed. These infinitely many branches accumulate on an envelope curve which passes through $k = 0.71435\ldots$ at $\delta = 1$ and corresponds to a limiting case of a solitary wave with an infinitely wide core.

All the branches start at $k = 1/2$, then veer off to larger k, and finally end at $k = 1/2$ again. At $k = 1/2$, these branches connect to the region of existence of gap solitary waves. Actually, the branches can be continued below $k = 1/2$ (into the spectrum's gap), where they correspond to a special subfamily of "superlocalized" gap solitons, whose tails decay at a faster rate than the generic exponential rate. That is, the linearization of (4) and (5) for k just smaller than $1/2$ gives rise to real eigenvalues $\pm\lambda_1$, $\pm\lambda_2$, say, with $|\lambda_1| < |\lambda_2|$ (and $\lambda_1 \to 0$ as $k \to 1/2$). Generic solitary waves decay on the longer decay length corresponding to λ_1, whereas those which form the continuation of an ES branch decay like $\exp(2x)$. Since the focus of this work is on ESs, we shall not consider their connection to gap solitons any further.

Recall that, in the present case ($q = 1$), $k > 1/2$ is a part of the continuous spectrum, cf. Eq. (6), thus, all the solitons corresponding to the solution branches shown in Fig. 2 indeed reside inside the continuous spectrum. To display the profiles of these ESs, we take $\delta = 1$. Then the first four k-values for ESs are 0.69625946 , 0.71369872, 0.71431982 and 0.714346946 , respectively. The corresponding ESs are shown in Fig. 3. As one can see, at the first k-value, both U and V solutions are single-humped. Following the usual convention [23], we call such ESs "fundamental". At other k-values, the ESs are multi-humped. This feature turns out to be true for all the embedded-soliton solutions found in the present model: every soliton belonging to the lowest branch of Fig. 2 is fundamental, while every soliton belonging to the other branches is multi-humped. The energy

$$E \equiv \int_{-\infty}^{+\infty} (|u|^2 + 2|v|^2)\, \mathrm{d}t \tag{8}$$

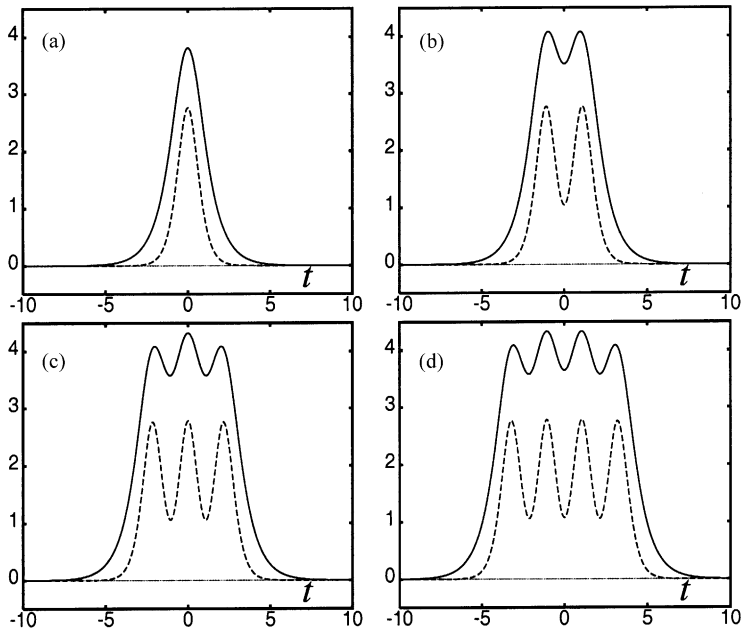

Fig. 3. The first four embedded solitons for $q = 1$ and $\delta = 1$ (see Fig. 2). The k-values are given in the text.

of the multi-humped ES always turns out to be higher than that of the fundamental ES for the same values of the parameters. Along each ES branch in Fig. 2, the solitary-wave's profile changes continuously. On all the branches, when δ is small, the SH (V) amplitude is larger than the FH (U) one. However, as δ increases, the U amplitude eventually outgrows the V amplitude (see Fig. 3).

A similar situation has been found for the case $\delta < 0, \gamma_{1,2} > 0$, which corresponds to the physical situation where the dispersion has the same sign at both harmonics, the cubic nonlinearity being self-focusing. Rather than plotting ES branches in the (δ, k)-plane, we choose instead to represent them in the (δ, q) plane for a typical value $k = 0.3$. Two such branches are displayed in Fig. 4. Some qualitative features of these solution branches can be noticed. First, the depicted branches end for low q at precisely the value $q = 0.6 \equiv 2k$, at which they could be continued (although we chose not to) into the gap-soliton region, as was the case for the branches in Fig. 2. Next, at the high q-end, the numerical evidence suggests that the branches can be continued up to $q = \infty$, approaching asymptotically the constant δ-values $-1.55\ldots$ and $-0.48\ldots$. There are some numerical difficulties in computing to arbitrarily high q (we note that values of $q = 40$ are not likely to be physically relevent) since the system of Eqs. (4) and (5) becomes stiff as the frequency of the continuous spectrum becomes very large. Nevertheless, the numerical evidence indicates that the U-component remains finite as $q \to \infty$, with the amplitude of the V-component tending to zero. Further, note from the insets in Fig. 4 that, for large q, both ES solutions appear to be single-humped (fundamental). But upon decreasing q, where the amplitudes of both U and V become larger, it is apparent that, while the left branch indeed represents a fundamental soliton, the solution corresponding to the right branch is non-fundamental, since it features "ripples" superimposed onto the central trough in the V component. Finally, we remark that only this nonfundamental branch passes through the physically

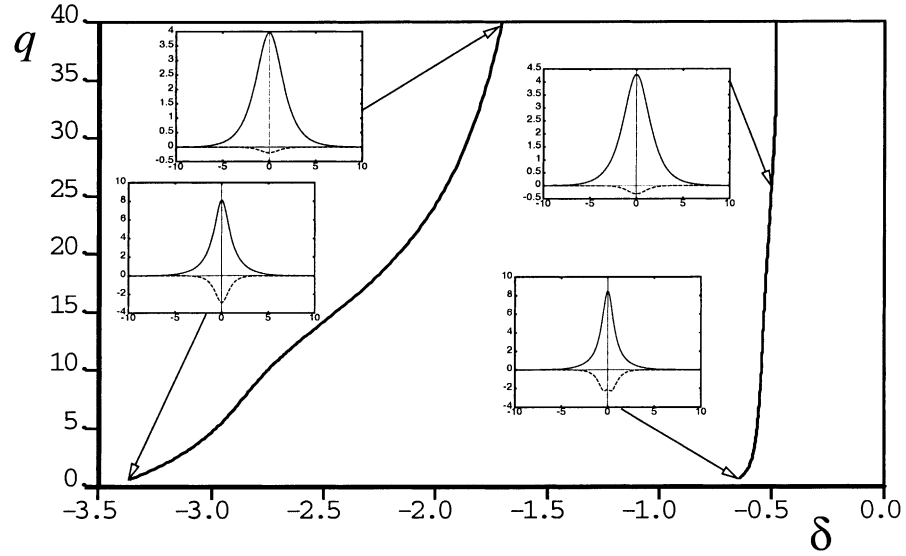

Fig. 4. Two branches, in the (δ, q) plane, of ES solutions for the second-harmonic generation model (1) and (2) with $k = 0.3$ and $\gamma_1 = \gamma_2 = 0.05$. The insets depict the profiles of $U(t)$ (positive component) and $V(t)$ (negative one) at various points along the branches.

significant value $\delta = -1/2$, corresponding to the model in the spatial domain (see above). In other words, it appears that the model in the spatial domain does not support a fundamental ES (see also below).

We should stress that, although the values of k which give rise to the exactly localized ESs were found with a finite accuracy, their existence can be proved rigorously. To this end, we define the minimum amplitude $R_{\min}(k)$ of the tail (7) as a result of minimization of $R(k, \phi_0)$ in the phase shift ϕ_0. The numerical data clearly show that the continuous curve $R_{\min}(k)$ does cross the zero axis. With regard to this, in a vicinity of the value k_1 that gives rise to the single-humped ES, we may postulate an expansion for the tail's amplitude (R' being a constant), that will be used below:

$$R_{\min}(k) = R'(k - k_1) + \mathrm{O}(k - k_1)^2. \tag{9}$$

2.2. A simplified model

As an analytically tractable example that explicitly proves the existence of an isolated single-humped ES for both positive and negative δ, we consider an approximation to Eqs. (1) and (2) in the limit when the SH component is much weaker than the FH one:

$$iu_z + \left(\tfrac{1}{2}\right) u_{tt} + u^* v + \gamma_1 |u|^2 u = 0, \tag{10}$$

$$iv_z - \left(\tfrac{1}{2}\right) \delta v_{tt} + qv + \left(\tfrac{1}{2}\right) u^2 + 4\gamma_2 |u|^2 v = 0. \tag{11}$$

The linearization of these equations generates the same continuous spectrum (6) as before, and for this system one can find the following exact single-humped ES at a single value of the propagation

constant

$$u = A\,\mathrm{e}^{ikz}\mathrm{sech}(\sqrt{2k_0}t),\ v = B\,\mathrm{e}^{2ikz}\mathrm{sech}^2(\sqrt{2k}t), \tag{12}$$

$$k = \tfrac{1}{4}(1+2\delta)^{-1}[2q - 3\delta(4\gamma_2 + 3\delta\gamma_1)^{-1}], \tag{13}$$

$$B = 2k\left(\frac{1+3\delta\gamma_1}{4\gamma_2}\right),\ A^2 = -\left(\frac{3\delta}{2\gamma_2}\right)k. \tag{14}$$

It is easy to show that, for $\delta > 0$ and $\gamma_{1,2} < 0$, this solution is always an ES (i.e. k belongs to the continuous spectrum), provided that

$$\left(\frac{3\delta}{2}\right)(4\gamma_2 + 3\delta\gamma_1)^{-1} < q < -\left(\frac{3}{4}\right)(4\gamma_2 + 3\delta\gamma_1)^{-1}. \tag{15}$$

This exact solution to the reduced model (10) and (11) can also be used to demonstrate the existence of ESs in the case $\delta < 0$. In that case, a condition for the existence of the solution, i.e. $k > 0$ and $A^2 > 0$ (see Eq. (14)) tells us, first of all, that it is necessary to have $\gamma_2 > 0$, which is exactly opposite to what was necessary in the case $\delta > 0$. Next, analyzing the condition that the propagation constant (13) belongs to the continuous spectrum, it is necessary to distinguish two different generic subcases (i) $0 < -\delta < 1/2$, and (ii) $-\delta > 1/2$. One finds that in case (i), the mismatch parameter must belong to the interval (cf. Eq. (15))

$$\left(\frac{3}{4}\right)(4\gamma_2 + 3\delta\gamma_1)^{-1} < q < \left(\frac{-3\delta}{2}\right)(4\gamma_2 + 3\delta\gamma_1)^{-1}, \tag{16}$$

while in case (ii), it must belong to the interval

$$\left(\frac{-3\delta}{2}\right)(4\gamma_2 + 3\delta\gamma_1)^{-1} < -q < \left(\frac{3}{4}\right)(4\gamma_2 + 3\delta\gamma_1)^{-1}. \tag{17}$$

A condition for the self-consistency of these double inequalities is, in both cases,

$$\gamma_1 > \left(\frac{4}{3|\delta|}\right)\gamma_2, \tag{18}$$

i.e. both Kerr coefficients must be positive.

An exact solution in the form (12), of this simplified system can also be found in the above-mentioned special case $\delta = -1/2$, corresponding to the spatial domain. In this case, the exact solution is very different from that in the generic case: it exists at a single value of the mismatch parameter

$$q_0 = -\left(\tfrac{3}{2}\right)(8\gamma_2 - 3\gamma_1)^{-1}, \tag{19}$$

i.e. it is structurally unstable, but it is not isolated in terms of k; instead, it exists for all positive k, being embedded in the region $k < q_0/2$ (which implies $q_0 > 0$, i.e. $\gamma_1 > (8/3)\gamma_2$, cf. Eq. (18)). The amplitudes of this exact solution for the case $\delta = -1/2$ are $A^2 = 3k/4\gamma_2$ and $B = 2k(1 - 3\gamma_1/8\gamma_2)$, cf. Eq. (14).

The existence of this degenerate family of exact single-humped solutions to the simplified model at $\delta = -1/2$ raises the question of whether a similar solution exists to the full model (1) and (2) in the same physically important case $\delta = -1/2$. In an attempt to find the latter solution by means of the continuation

procedure starting from the simplified model, we have introduced an intermediate model with an auxiliary parameter G,

$$iu_z + \left(\tfrac{1}{2}\right) u_{tt} + u^* v + \gamma_1(|u|^2 + 2G|v|^2)u = 0, \tag{20}$$

$$iv_z - \left(\tfrac{1}{2}\right) \delta v_{tt} + qv + \left(\tfrac{1}{2}\right) u^2 + 2\gamma_2(G|v|^2 + 2|u|^2)v = 0. \tag{21}$$

Obviously, $G = 0$ and $G = 1$ correspond, respectively, to the simplified and full models. The continuation procedure was performed in the same way as mentioned above, this time in the pair of parameters (G, q) for a fixed value of k, starting from the point $(G = 0, q = q_0)$, where the above exact solution is available, with q_0 given by Eq. (19).

A preliminary numerical investigation shows that the continuation of these ES solutions is possible, up to some finite G-value which depends on k, but it is always < 1. Actually, the branch of the single-humped soliton solutions can be continued to still larger G, but the solitons cease to be embedded, crossing into the spectral gap (nevertheless, they remain physically meaningful solutions). Another essential result is that, at any finite G in Eqs. (20) and (21), the degeneracy of the exact solutions to the simplified model (the one with $G = 0$) is lifted: for $G \neq 0$ the solutions exist in a finite interval of values of q, rather than at a single value (cf. Eq. (19)), and they are again isolated in terms of k, rather than forming a continuous family. Results of a more detail numerical investigation will be presented elsewhere.

3. Stability of the embedded solitons

The stability of ESs is a crucial issue for their physical application. The simulations (see below) demonstrate that all the fundamental (single-humped) ESs have no exponentially growing instability. However, they are subject to a weak (sub-exponential) instability. Below, we explain that this semi-instability is due to the fact that an ES is an isolated solution, as the values of k that give rise to the ESs are discrete. The corresponding energies of the ESs are therefore, discrete too. On the other hand, any generic small perturbation of an ES will tend to transform it into an adjacent state, which is a delocalized soliton with a nonvanishing tail in the SH component. However, both systems considered above, (1) and (2) and (10) and (11), conserve the energy E defined by Eq. (8). Thus, it would take an infinite amount of energy to create a nonvanishing tail, regardless of its amplitude. Consequently, there are two possibilities. First, if the initial perturbed state has a total energy which is less than that of the unperturbed ES, E_1, the energy lost in an attempt to generate the infinite tail drives the soliton farther away from the initial ES state. As a result of this, the perturbed ES can be expected to eventually decay into radiation. On the other hand, if the initial perturbed state has larger energy than E_1, we may expect that the energy loss through the tail generation would drag the central body back toward the unperturbed ES, meanwhile shedding off the excess energy as radiation. Eventually, the pulse would reestablish itself into the original ES, with a fading emission of radiation. We call such a perturbation nondestructive. Thus, we anticipate that the fundamental ES will be subject to a one-sided instability that must necessarily be subexponential. We call such an object semistable.

To achieve a qualitative understanding of this semistability, we assume that the only decay channel available to this ES is through the transformation into a delocalized soliton, as was outlined above. Assum-

ing a partially formed tail with a finite length and the amplitude $R_{\min}$ defined above, it is straightforward to write down the rate at which the soliton is losing energy, pumping it into the growing tail:

$$\frac{\mathrm{d}E}{\mathrm{d}z} = -CR_{\min}^2 V_{\mathrm{g}}, \tag{22}$$

where the tail's growth rate $V_{\mathrm{g}} = \mathrm{d}t/\mathrm{d}z$ is the inverse linear group velocity for a given k, which can be easily found from the model's dispersion relation, and C is some constant. By definition, the expression CV_{g} is positive.

In the present model, Eq. (2) yields the dispersion relation for the SH waves

$$2k = q + \left(\tfrac{1}{2}\delta\right)(2\omega)^2, \tag{23}$$

where 2ω is the frequency. This equation produces the following expression for the inverse group velocity

$$V_{\mathrm{g}}^2 \equiv \left[\frac{\mathrm{d}(2k)}{\mathrm{d}(2\omega)}\right]^2 = 2\delta\left(\frac{k-q}{2}\right). \tag{24}$$

The remaining central body of the soliton is, essentially, the same as that of the delocalized soliton, corresponding to a slowly varying $k(z)$. Since the energy of the delocalized-soliton's central body is a function of k and vice versa, we expand $k - k_1 \approx k'(E - E_1)$ (cf. Eq. (9)), where k' is a constant, and $k_1 \equiv k(E_1)$. Substituting this into the above Eq. (9) , and the resulting expression for $R_{\min}$ into Eq. (22), we obtain

$$\frac{\mathrm{d}(E - E_1)}{\mathrm{d}z} = -CV_{\mathrm{g}}(R'k')^2(E - E_1)^2. \tag{25}$$

The solution to Eq. (25) is

$$E(z) = E_1 + (E_0 - E_1)[1 + CV_{\mathrm{g}}(R'k')^2(E_0 - E_1)z]^{-1}, \tag{26}$$

where E_0 is the initial energy of the perturbed pulse. Eq. (26) shows that the perturbation slowly (algebraically) decays as $z \to \infty$, if $E_0 > E_1$. This corresponds to the stable side of the semistable ES. On the other hand, if $E_0 < E_1$, the energy slowly (algebraically, rather than exponentially, as was said above) decays to zero, (formally) reaching zero at a finite value of z. This shows the unstable side of the semistability. Although Eqs. (25) and (26) are rigorously valid only when the perturbed pulse is close to the ES, the above predictions have been verified by our numerical simulations (see below).

To verify these predictions, we numerically simulated the evolution of deliberately perturbed ESs in the framework of Eqs. (1) and (2). The initial condition was taken, for instance, as

$$u(0,t) = U(t) + c_1\,\mathrm{sech}(2t), \quad v(0,t) = V(t) + c_2\,\mathrm{sech}(2t), \tag{27}$$

where (U, V) is the ES proper, and $c_{1,2}$ are small amplitudes of the disturbance. We first consider the fundamental ES taken from Fig. 3 a, adding to it the perturbation with $c_1 = c_2 = 0.1$, so that the energy of this perturbed state is $> E_1$. The result is shown in Fig. 5. We see that, as z increases, the pulse slightly adjusts itself, with the amplitudes of its two components very slowly decreasing towards those of the unperturbed ES, which are 3.8099 and 2.7603, respectively. Closer examination of the evolution of the v-component shows that, as z increases, it develops small long symmetric tails (no such tails are present in the u-component). The data show that these tails have a dominant frequency $\omega \approx 0.88$. For $\omega = 0.88$, the SH dispersion relation (23) yields $k \approx 0.6936$, which is very close to the wavenumber k_1 of the unperturbed ES. From Eq. (24), we further find the corresponding value of the inverse group velocity,

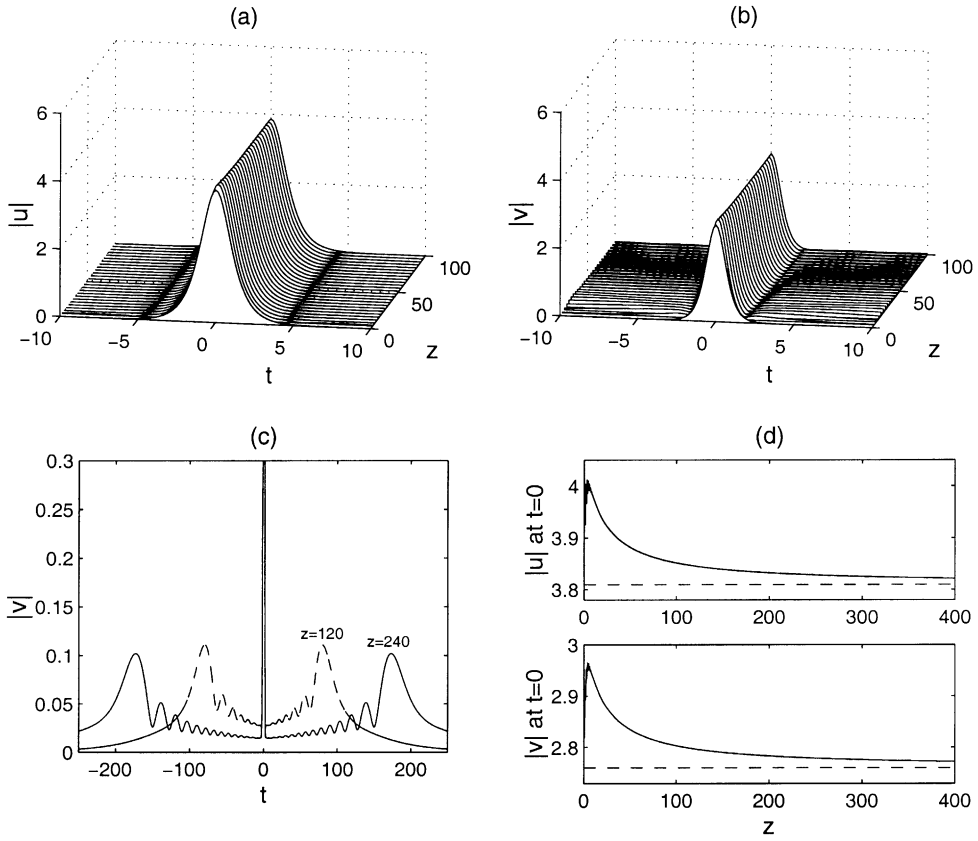

Fig. 5. Evolution of the fundamental embedded soliton (corresponding to Fig. 3a) initiated by the nondestructive perturbation, with $c_1 = c_2 = 0.1$, in the initial conditions (27). The dashed lines in (d) are the amplitudes of the u- and v-components of the unperturbed soliton, which are 3.8099 and 2.7603, respectively.

$V_g = 0.88$, which must be the speed at which the v-tail propagates away from the central pulse, see above. This prediction agrees as well with the numerical results. Lastly, we notice that the amplitude of the tail decreases in z (see Fig. 5(c)), as the energy supply ceases due to the restabilization of the central pulse.

Next, we take the initial condition (27) with $c_1 = c_2 = -0.1$. Then the perturbed initial state has energy $< E_1$. The numerical evolution in this case is shown in Fig. 6. The v-component develops tails whose amplitude grows as z increases, because the central body of the pulse continually deviates further away from the fundamental ES. Eventually, the perturbed soliton perishes as predicted. After the decay, we observe that the u-component completely decays, while v evolves into separate solitary pulses and radiation. This can be easily understood since, when $u = 0$, Eq. (2) reduces to the well-known nonlinear Schrödinger (NLS) equation.

The situation is basically the same when $\delta < 0$: positive energy perturbations are safe, while negative energy perturbations trigger the decay of ES. However, as we shall see below, for $\delta < 0$ this decay seems to be much slower than that found above for $\delta > 0$. Numerically, we simulated the system (1) and (2), with the initial condition (27). Here, $U(t)$ and $V(t)$ is the ES solution corresponding to the left branch in Fig. 4 (the parameters are $\delta = -2.9292$, $q = 6.0556$, $k = 0.2936251$ and $c_1 = c_2 = 0.05$). Figs. 7 and 8

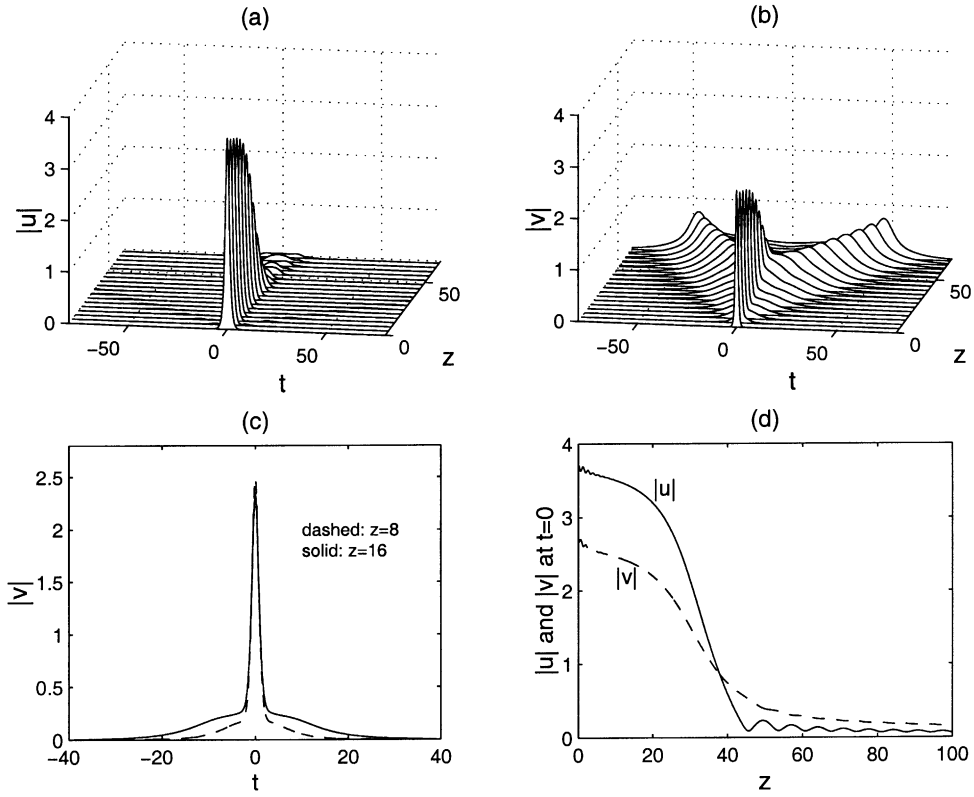

Fig. 6. Evolution of the fundamental embedded soliton (corresponding to Fig. 3a) initiated by the destructive perturbation, with $c_1 = c_2 = -0.1$ in the initial conditions (27).

depict, respectively, the effects of the positive-energy and negative-energy perturbations. In both cases, we observe fast oscillations on top of slow ones in the evolution of $|u|$ and $|v|$ at $t = 0$. These oscillations are very similar to those reported in [25] for perturbed solitons in the standard second-harmonic-generation system with no cubic nonlinearity (note that those solitons were regular ones, rather than ESs). In that case, the slow oscillations were attributed to an internal mode, while the fast oscillations were construed as a result of beatings between the internal mode and a quasi-mode. This quasi-mode is localized in the FH component, but resonates with the continuous spectrum in the SH component. Both oscillations were found in the simulations, and they last for a very long time, even though they were theoretically expected to eventually decay due to a very weak radiation damping.

We believe that similar mechanisms are also at work in our model, in both cases shown in Figs. (7) and (8). However, a difference is that the solitons in our model are embedded, while those in the model considered in Ref. [25] were not. On the other hand, there are important similarities because perturbations of ES naturally resonate with the continuous spectrum of the SH component, which is expected to eventually (through a presumably existing quasi-mode) give rise to the slow beatings, which are indeed observed in the present simulations. On the other hand, we must note that the ES's internal modes, whose existence is suggested by the long-lasting slow oscillations in Figs. 7 and 8, cannot be internal modes of the same type as those known in regular gap solitons [25]. Indeed, in order that an internal localized

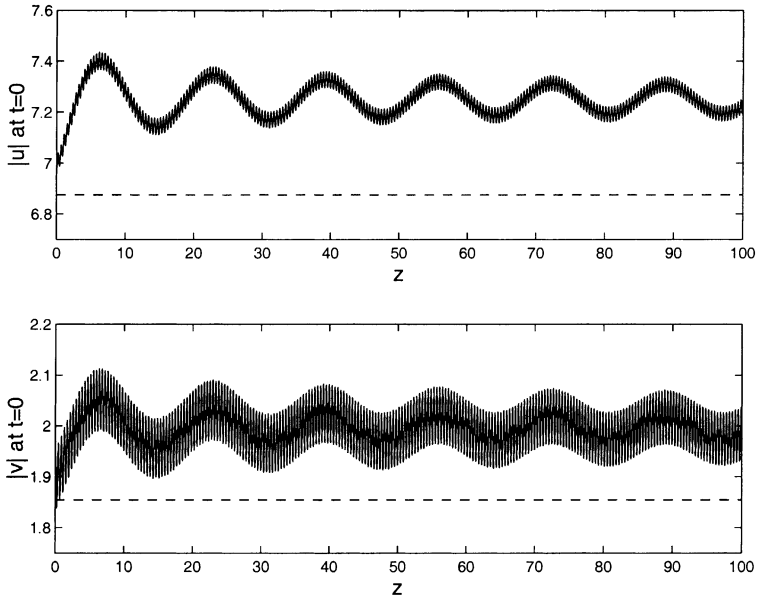

Fig. 7. Evolution of a perturbed soliton with positive energy perturbation ($c_1 = 0.1$, $c_2 = -0.1$ in (27)) for (1) and (2) from the left-hand fundamental branch of Fig. 4.

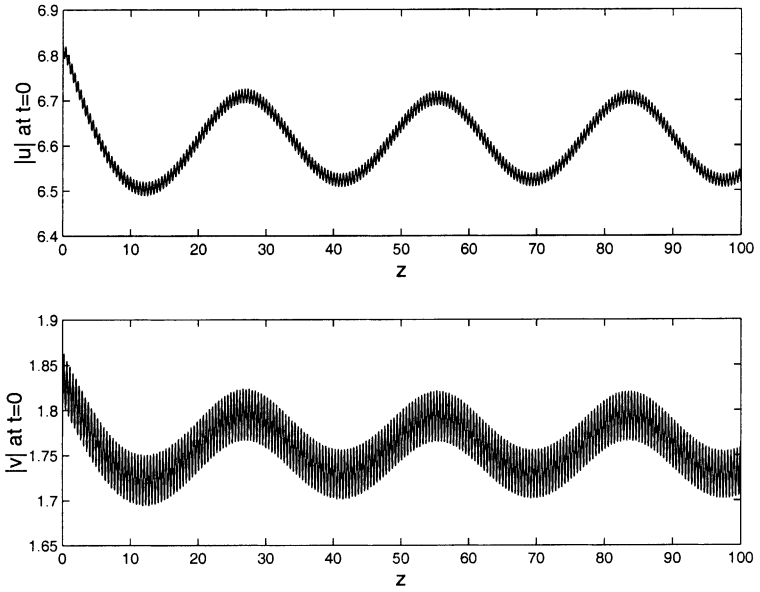

Fig. 8. Evolution of a perturbed soliton with a negative energy perturbation ($c_1 = -0.05$, $c_2 = 0.05$ in Eq. (27)) in the model (1) and (2). The soliton belongs to the left-hand fundamental branch in Fig. 4.

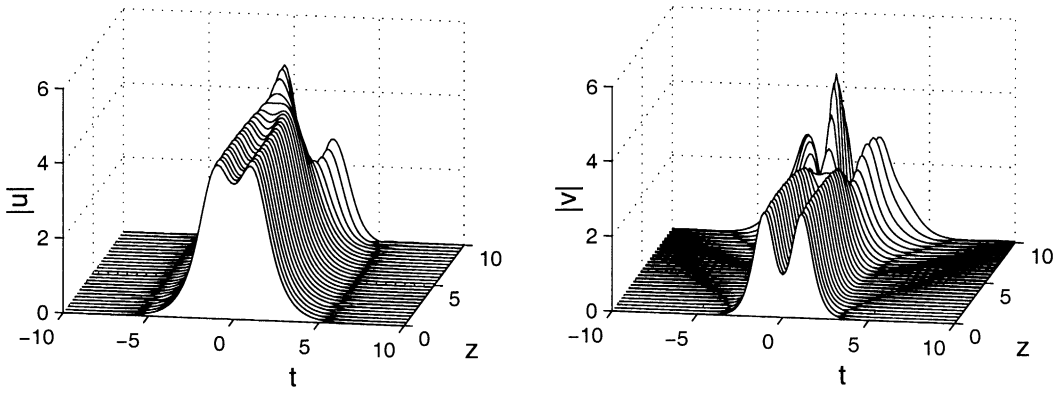

Fig. 9. Instability of the double-humped embedded soliton (corresponding to Fig. 3b). Here, $c_1 = c_2 = 0.1$ in the initial conditions (27).

mode exists, there must be enough free parameters in the tails of the modes, so that by adjusting these parameters, one can get an internal localized mode. But in the linearized equation around any embedded soliton, there are just not enough free parameters in the tails. Nevertheless, one does see very persistent oscillations in Figs. 7 and 8.

Although according to the semistability argument, an ES with a negative-energy perturbation, like that shown in Fig. 8, would eventually decay, in the simulations, the decay turns out to be extremely slow in the case $\delta < 0$. Detailed examination of the numerical solutions shows that the central pulse (the v component) in Fig. 8 indeed keeps shedding oscillating tails into the far field. However, the observed tail amplitudes turn out to be extremely small ($\lesssim 0.001$ or smaller). This is why the expected decay of the perturbed ES is not, as a matter of fact, seen at all in this figure. Because of this, the actually observed evolution is dominated by the internal vibrations, just as in Fig. 7 with a positive perturbation, and as in the above-mentioned work [25]. It would take an extremely long propagation distance for the pulse in Fig. 8 to show a tangible decay. As a result, the ESs in the present model with $\delta < 0$ are virtually stable, when compared to the previously considered $\delta > 0$ case [31], where the semi-instability was a tangible feature. The virtual stability of ES for $\delta < 0$ is a new result reported in the present paper, and its importance is quite obvious.

Concerning the higher-order (multi-humped) ESs, in nearly all the known nonlinear-optical models related to the present one they are strongly unstable [39–42] (although double-humped solitons were numerically found to be as stable as the single-humped ones in a three-wave second-harmonic-generation gap-soliton model [38]). We simulated the stability of the double-humped ES shown in Fig. 3. The evolution of its perturbed state (27) with $c_1 = c_2 = 0.1$ is displayed in Fig. 9. We see that, as expected, the soliton quickly loses its integrity. To clarify this instability, we have also numerically investigated the linearization of Eqs. e1,e2 around this soliton, and found linearly unstable (i.e. exponentially growing) modes. Thus, unlike the semistable fundamental ES, the multi-humped one is quickly destroyed by a perturbation. We have also carried out numerical stability analysis of the multi-humped ES belonging to the right branch in Fig. 4, the results of which are shown in Fig. 10. One can see the onset of a violent exponential instability, followed by the relaxation of the solution towards a bounded oscillating state. We have also verified that a numerical study of the linearization of Eq. (1) and (2) about this multi-humped ES does produce exponentially unstable eigenmodes.

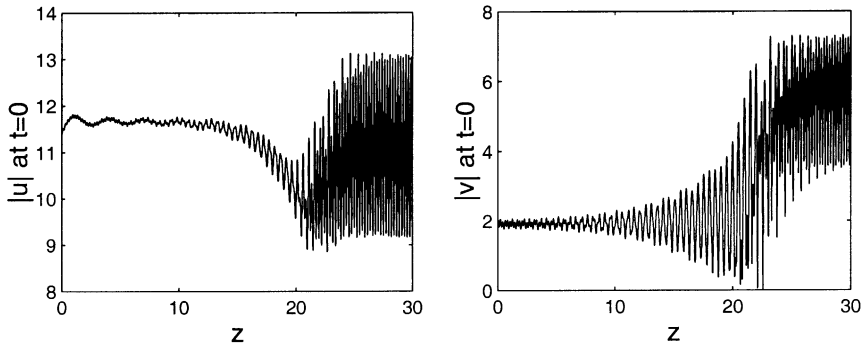

Fig. 10. The linear instability and subsequent nonlinear evolution of a perturbed embedded soliton belonging to the right-hand branch in Fig. 4 for $\delta = -0.5$, $\gamma_1 = \gamma_2 = 0.05$, $q = 10$ and $k = 1.9298$. The initial condition is given by (27) with $c_1 = 0.1$ and $c_2 = -0.1$.

In view of these results, we conjecture the following. In Hamiltonian systems, fundamental ESs are, in general, linearly stable but nonlinearly semi-stable. The higher-order ESs (which usually have internal ripples in their profiles) are, generally, linearly unstable. Preliminary results for the extended 5th-order KdV equation indicate qualitatively the same properties. This would also agree with previous numerical results for a higher-order NLS equation, wherein the results may be interpreted as saying that an isolated fundamental ES [33] was semi-stable, whereas the multi-humped ones [32] were exponentially unstable. Recently, the semi-stability of fundamental ESs in the extended Hamiltonian KdV equations has been shown analytically in [18].

It should be noted that, besides ESs and the above-mentioned degenerate NLS solitons, Eqs. (1) and (2) also support the ordinary gap solitons when $\delta > 0$ and $q > 0$. In this case, we have found that the spectrum gap $0 < k < q/2$ is completely filled. In addition, these gap solitons are not unique (at a given value of k), all being multi-humped. Not surprisingly (because of their multi-humpedness), all these gap solitons were found to be linearly unstable. This circumstance lends an additional relevance to the ES solutions existing at the same values of the parameters, which suffer only from the weak nonlinear semi-instability.

4. Conclusion

In this paper, we have established the existence of embedded solitons in a second-harmonic-generation system with competing quadratic and cubic nonlinearities. We heuristically argued that the fundamental embedded solitons must be linearly stable and nonlinearly semi-stable. These predictions were confirmed by direct numerical simulations. For the case of anomalous dispersion for both harmonics, the simulations have revealed that the fundamental embedded solitons are virtually stable. However, in the version of the model corresponding to the spatial domain, only unstable multi-humped embedded solitons were found.

It is necessary to stress that the existence of ES in Eqs. (1) and (2) is by no means an isolated phenomenon. In fact, such objects have also been identified in the dispersively perturbed massive Thirring model [36], three-wave-interaction model [29], an extended KdV system [18,34,37], an extended NLS equation [32,33], a coupled KdV system [35], etc. We believe that the embedded solitons are a generic object in nonlinear wave systems which have at least two different branches in their linear spectrum, and have the potential for future application, for example in all-optical switching.

Acknowledgements

We appreciate a useful discussion with Y. Kivshar. J.Y. acknowledges a partial financial support from NSF and AFOSR. The research of D.J.K. has been supported in part by the AFOSR. B.A.M. appreciates a Benjamin Meaker visitor's fellowship provided by the University of Bristol.

References

[1] M. Remoissenet, Waves Called Solitons, Springer-Verlag, New York, 1994.
[2] C.M. de Sterke, J.E. Sipe, Progr. Opt. 33 (1994) 203.
[3] C. Conti, S. Trillo, G. Assanto, Phys. Rev. Lett. 78 (1997) 2341.
[4] H. He, P.D. Drummond, Phys. Rev. Lett. 78 (1997) 4311.
[5] T. Peschel, U. Peschel, F. Lederer, B.A. Malomed, Phys. Rev. E 55 (1997) 4730.
[6] A. Kozhekin, G. Kurizki, Phys. Rev. Lett. 74 (1995) 5020.
[7] B.I. Mantsyzov, Phys. Rev. A 51 (1995) 4939.
[8] A.E. Kozhekin, G. Kurizki, B.A. Malomed, Phys. Rev. Lett. 81 (1998) 3647.
[9] D.J. Kaup, B.A. Malomed, JOSA B 15 (1998) 2838–2846.
[10] B.J. Eggleton, R.E. Slusher, C.M. de Sterke, P.A. Krug, J.E. Sipe, Phys. Rev. Lett. 76 (1996) 1627.
[11] Y. Pomeau, A. Ramani, B. Grammaticos, Physica D 31 (1988) 127.
[12] V.I. Karpman, Phys. Rev. E 47 (1993) 2073.
[13] J.P. Boyd, Physica D 48 (1991) 129.
[14] R. Grimshaw, N. Joshi, SIAM J. Appl. Math. 55 (1995) 124.
[15] T.R. Akylas, T.S. Yang, Stud. Appl. Math. 94 (1995) 1.
[16] T.S. Yang, T.R. Akylas, Phys. Fluids 8 (1996) 1506.
[17] T.S. Yang, T.R. Akylas, J. Fluid Mech. 330 (1997) 215.
[18] J. Yang, Dynamics of embedded solitons in the extended KdV equations. Stud. Appl. Math. Vol 106, 337 (2001).
[19] D.J. Kaup, T.I. Lakoba, B.A. Malomed, J. Opt. Soc. Am. B 14 (1997) 1199.
[20] P.K.A. Wai, H.H. Chen, Y.C. Lee, Phys. Rev. A 41 (1990) 426.
[21] S. Trillo, A.V. Buryak, Y.S. Kivshar, Opt. Comm. 122 (1996) 200.
[22] O. Bang, Y.S. Kivshar, A.V. Buryak, Opt. Lett. 22 (1997) 1680.
[23] G.P. Agrawal, Nonlinear Fiber Optics, Academic Press, New York, 1995.
[24] A. Capobianco, B. Costantini, C. De Angelis, A. Laureti Palma, C.F. Nalesso, J. Opt. Soc. Am. B 14 (1997) 2602.
[25] C. Etrich, U. Peschel, F. Lederer, B.A. Malomed, Phys. Rev. A 52 (1995) R3444.
[26] L. Torner, D. Mazilu, D. Mihalache, Phys. Rev. Lett. 77 (1996) 2455.
[27] C. Etrich, U. Peschel, F. Lederer, B.A. Malomed, Phys. Rev. E 55 (1997) 6155.
[28] A.R. Champneys, B.A. Malomed, J. Phys. A 32 (1999) L547–L553.
[29] A.R. Champneys, B.A. Malomed, Phys. Rev. E 61 (2000) 886–890.
[30] P. Di Trapani, D. Caironi, G. Valiulis, A. Dubietis, R. Danielius, A. Piskarskas, Phys. Rev. Lett. 81 (1998) 570.
[31] J. Yang, B.A. Malomed, D.J. Kaup, Phys. Rev. Lett. 83 (1999) 1958.
[32] A.V. Buryak, Phys. Rev. E 52 (1995) 1156.
[33] J. Fujioka, A. Espinosa, J. Phys. Soc. Jpn. 66 (1997) 2601.
[34] S. Kichenassamy, P.J. Olver, SIAM J. Math. Anal. 23 (1992) 1141.
[35] R. Grimshaw, P. Cook, in: A.T. Chwang, J.H.W. Lee, D.Y.C. Leung (Eds.), Proceedings of the Second International Conference on Hydrodynamics, Hong Kong, 1996, p. 327.
[36] A.R. Champneys, B.A. Malomed, M.J. Friedman, Phys. Rev. Lett. 80 (1998) 4168.
[37] A.R. Champneys, M.D. Groves, J. Fluid Mech. 342 (1997) 199.
[38] W.C.K. Mak, B.A. Malomed, P.L. Chu, Phys. Rev. E 58 (1998) 6708.
[39] J. Yang, Stud. Appl. Math. 96 (1996) 111.
[40] J. Yang, Physica D 108 (1997) 92.
[41] M.I. Weinstein, Comm. Pure Appl. Math. 39 (1986) 51.
[42] Y. Silberberg, Y. Barad, Opt. Lett. 20 (1995) 246.